Computer modelling and numerical simulation of the solid state diode pumped Nd:YAG laser with intracavity saturable absorber

Yuriy Yashkir

Yashkir Consulting

28. January 2009

Computer Modelling and Numerical Simulation of the Solid State Diode Pumped Nd:YAG Laser with Intracavity Saturable Absorber

Dr. Yuri Yashkir

yuri.yashkir@gmail.com; YASHKIR CONSULTING LTD.

Contents

1 Introduction

The model of a laser is based on the following assumptions. Laser consists of a laser output coupler (reflection R_p , with the spherical surface radius of curvature R_0), an active crystal (rod[1])a_c-long (refractive index ${n_c}^2$), a passive Q-switching element (a saturable absorber crystal[3] with initial transparency T_q , length a_{Cr}), and a HR back mirror (curvature radius R_m). The total length of the laser cavity is a. The laser rod is pumped with a set of laser diodes. Laser pump maximal power is P_D^{max} . Laser active ion lifetime is τ_n and the saturable absorber ion lifetime is τ_q . In this model it is assumed that all variables depend on $\vec{r}, t$ only ($\vec{r} = (x, y, 0)$, axis z is the cavity axis). Optical pump is given by $\Phi_D(\vec{r})$ (the two dimensional pump distribution) and $\sigma(t)$(pump pulse temporal shape). Methodology of laser intensity modeling and multi-dimentional light/matter interaction is based on previously published papers (Yashkir and Liu, 2006), (Yashkir, 2006a), (Yashkir, 2006b), (Yashkir and Yashkir, 2004), (Yashkir et al., 2004), (Yashkir, 2002), (Yashkir and van Driel, 1999).

[1] $Nd^{+3} : YAG$, $\tau_n = 230\mu s$
[2] $n_c = 1.818$
[3] $Cr^{4+} : YAG$, $\tau_q = 8.5\mu s$

2 Basic model equations

The laser cavity round trip time is denoted as T_p, and the reflection coefficient of the output coupler (mirror) is R_p . Photon losses in the laser cavity (not related to the saturable absorber) are described by the photon lifetime constant τ_{ph}. It can be identified as follows. During k round trips (time $t = kT_p$), the initial intracavity electromagnetic emission energy is reduced by a factor of R_p^k. From the obvious equation

$$R_p^{\frac{t}{T_p}} = e^{-\frac{t}{\tau_{ph}}} \tag{1}$$

we obtain

$$\tau_p = \frac{T_p}{\rho_p} \tag{2}$$

where parameter $\rho_p = -\mathbf{ln}R_p$ can be thought of as an average loss per round-trip (it may be different for different laser cavity modes). This approximation is valid, obviously, if the laser power changes slowly compared to the cavity round trip time:

$$\max_t \left| \frac{d}{dt} \mathbf{ln} P(t) \right| \ll \frac{1}{T_p} \tag{3}$$

For a laser pulse (pulse width τ_p) this criterion can be reduced to $\tau_p \gg T_p$.
The optical pumping of the laser rod can be estimated as follows. Diode pump energy at $[\vec{r}, t]$ in $[dV, dt]$ is given by the following expression:

$$d^2 E_D = P_D(t) \cdot \Phi_D(\vec{r}) \cdot dV \cdot dt, \tag{4}$$

where
$P_D(t)$ is total pump power,$\Phi_D(\vec{r})$ is the spatial distribution defined by the configuration setup of pumping sources assuming

$$\int \Phi_D(\vec{r}) dV = 1. \tag{5}$$

The fraction u of the pump energy absorbed in the laser crystal is assumed known. Then the number of absorbed photons dN_D (same as number dN_n of active excited ions) is equal to:

$$dN_n = \frac{u}{h\nu_D} dE_D. \tag{6}$$

The relative population factor change is then equal to

$$dn(\vec{r}, t) = \frac{dN_n}{dN_0} = \frac{u}{h\nu_D} \frac{dE_D}{c_0 dV} = u \frac{P_D(t)\Phi_D(\vec{r}) dV dt}{h\nu_D c_0 dV} = \frac{u}{h\nu_D c_0} P_D(t)\Phi_D(\vec{r}) dt \tag{7}$$

where c_0 is the concentration of active ions.

Taking into account the spontaneous decay of excited ions (time constant τ_n) we arrive to the rate equation for the relative population factor

$$\frac{dn(\vec{r},t)}{dt} = \frac{u}{h\nu_D c_0} P_D(t)\Phi_D(\vec{r})(1 - n(\vec{r},t)) - \frac{n(\vec{r},t)}{\tau_n}. \tag{8}$$

An estimation of the factor

$$\sigma = \frac{u}{h\nu_D c_0} \tag{9}$$

for a 1%-doped $Nd^{3+} : YAG$ crystal ($c_0 = 1.36{\cdot}10^{20} cm^{-3}$) pumped at $\lambda_D = 800nm$, assuming $u = 1$, is as follows:

$$\sigma^* = 3 \cdot 10^{-8} \frac{m^3}{J} \equiv 0.03 \frac{m \cdot m^3}{KW \cdot \mu s} \tag{10}$$

For simplicity assume that the pump distribution function is uniform along laser crystal ($0 \le z \le a$,$a = 1cm$) and it has the Gaussian shape in plane xy with the Gaussian diameter of $w_D = 1mm$:

$$\Phi_D(x,y,z) = \frac{2}{aw_D\sqrt{\pi}} e^{-4\frac{x^2+y^2}{w_D^2}} \tag{11}$$

Maximal value of $\Phi_D(x,y,z)$ is

$$\Phi_D(0,0,z) = \Phi_D^{max} = \frac{2}{aw_D\sqrt{\pi}} \approx 0.11(mm)^{-3} \tag{12}$$

Solution of the equation for $n(\vec{r},t)$ asymptotically tends to

$$n_\infty = \left(1 + (\sigma P_D \Phi_D^{max} \tau_n)^{-1}\right)^{-1} \tag{13}$$

Assuming pump power $P_D = 1KW$ and $\tau_D = 230\mu s$ we obtain $n_\infty \approx 0.43$. Dependence of n_∞ on the pump power has a typical shape:

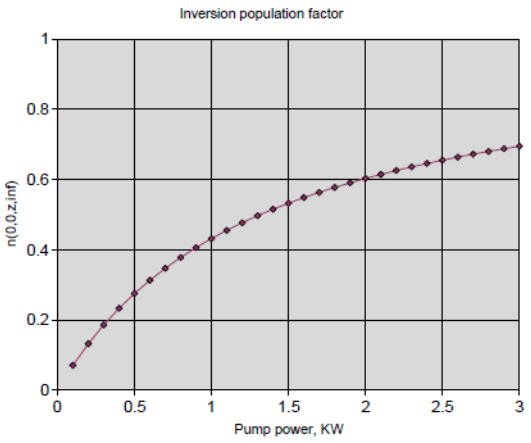

Figure 1: Inversion population factor dependence on the pumping power

It is important to note that laser crystal saturation effect due to optical pumping is not very significant at pump powers below $1KW$.

Stimulated emission of the excited ions is based on the probability of an ion to emit a photon during the time interval dt :

$$\mathbf{dB}_s = \sigma_s \frac{\mathbf{I}_p}{h\nu} dt, \tag{14}$$

where σ_s is the emission cross-section of an ion, $\mathbf{I}_p$ is the local light intensity, ν is the laser photon frequency.
Laser intracavity light consists of k_{max} modes ($N_p^{(k)}$ photons in each k^{th} mode). Spatial distribution of photons is $N_p^{(k)}\Phi_k(\vec{r})$, where all mode functions are orthogonal:

$$\int_{-\infty}^{\infty} \Phi_k(\vec{r})\Phi_n(\vec{r})dV = \delta_{kn}. \tag{15}$$

Therefore, the energy density in the vicinity of $(\vec{r}, t)$ is equal to

$$h\nu \sum_{k=1}^{k_{max}} N_p^{(k)}\Phi_k(\vec{r}), \tag{16}$$

and the intensity is equal to

$$\mathbf{I}_p = ch\nu \sum_{k=1}^{k_{max}} N_p^{(k)}\Phi_k(\vec{r}). \tag{17}$$

The average (expected) number of stimulated transitions of excited ions (equal to the number of stimulated photons added) in an elementary volume $dV \cdot dt$ is then as follows:

$$d^2N_p = -d^2N_n = n(\vec{r}, t)c_0 dV \mathbf{dB}_s = cc_0\sigma_s n(\vec{r}, t) \sum_{k=1}^{k_{max}} N_p^{(k)}\Phi_k(\vec{r})dVdt \tag{18}$$

It is convenient to introduce the value of

$$p_k(t) = \frac{N_p^{(k)}}{c_0 v_k}, \tag{19}$$

where $v_k = a_c\pi w_k^2$ is a k^{th} mode volume (w_k is the Gaussian mode width, and a_c is the length of the active crystal). The corresponding change of relative number of ions with downward transitions is equal then to

$$-\frac{dn(\vec{r}, t)}{dt} = -\frac{d^2N_n}{c_0 dVdt} = cc_0\sigma_s n(\vec{r}, t) \sum_{k=1}^{k_{max}} v_k p_k \Phi_k(\vec{r}). \tag{20}$$

We introduce now the parameter $\chi = cc_0\sigma_s$ and then we add the above expression to the rate equation for $n(\vec{r},t)$. It is:

$$\frac{dn(\vec{r},t)}{dt} = \sigma_D P_D(t)\Phi_D(\vec{r})(1-n(\vec{r},t)) - \chi n(\vec{r},t)\sum_{k=1}^{k_{max}} v_k p_k(t)\Phi_k(\vec{r}) - \frac{n(\vec{r},t)}{\tau_n}. \quad (21)$$

where $\sigma_D = u/(h\nu c_0)$. Using this equation the total number of emitted photons per dt ($dN_p = \int_V d^2N_n$) can be calculates as

$$dN_p \equiv \sum_{k=1}^{k_{max}} dN_p^{(k)} = cc_0\sigma_s \sum_{k=1}^{k_{max}} N_p^{(k)} \int\limits_V n(\vec{r},t)\Phi_k(\vec{r})dVdt. \quad (22)$$

Assuming that photons in each mode cause stimulated emission into the same mode only, and that photons in each mode comes from all elementary volumes of the laser crystal we can write the following rate equation for $p_k(t)$:

$$\frac{dp_k}{dt} = \chi p_k \int\limits_{-\infty}^{\infty} n(\vec{r},t)\Phi_k(\vec{r})dV - p_k\frac{\rho_p}{T_p}. \quad (23)$$

Intracavity losses are accounted by the factor τ_p. The photon losses due to the absorption in a saturable absorber (during dt) are introduced as follows. Absorption coefficient is equal to $\alpha_q = c_q\sigma_q$ (where c_q and σ_q are concentration and absorption cross section of absorbing ions of the saturable absorber crystal). During one round trip (time T_p) the intracavity light density (photon flux) $p_k(t)\Phi_k(\vec{r})$ is reduced by the factor of $e^{-2\alpha_q a_q}$ which is equivalent to the additional member of the rate equation for

$$\frac{dp_k}{dt}\Phi_k(\vec{r}) = \cdots - p_k\Phi_k(\vec{r})\frac{2\alpha_q a_q}{T_p}(1-q(\vec{r},t))\cdots. \quad (24)$$

Here a_q is the length of the satuarable absorber, and q is the relative number of excited ions in the saturable absorber crystal (absorption takes place only from the ground state). It is convenient to use the following formula $\alpha_q a_q \equiv -\ln T_q$ (value T_q is a one-path transparency of the crystal). Residual absorption of the crystal due to absorption from excited levels is introduced the same way:

$$\frac{dp_k}{dt}\Phi_k(\vec{r}) = \cdots - p_k\Phi_k(\vec{r})\frac{2\alpha_q a_q}{T_p}(1-q) - p_k\Phi_k(\vec{r})\frac{2\gamma_q a_q}{T_p}q\cdots. \quad (25)$$

Integration by $dV \equiv d^2\vec{r}$ gives, finally, the rate equation for photon dynamics

$$\frac{dp_k}{dt} = \chi p_k \int\limits_V n(\vec{r},t)\Phi_k(\vec{r})dV - \frac{p_k}{T_p}\left(\rho_p + 2a_q\left[\alpha_q(1 - \int\limits_V q(\vec{r},t)\Phi_k(\vec{r})dV) + \gamma_q \int\limits_V q(\vec{r},t)\Phi_k(\vec{r})dV\right]\right) \tag{26}$$

The rate equation for excitation dynamics of active ions of a saturable absorber is derived using the following considerations. The number of excited ions in a volume $dVdt$ is $dN_q = \frac{dE_p}{h\nu}$, where the absorbed light energy is the product of the light energy stored in the volume dV and the absorption rate during time dt :

$$dE_p = \left[h\nu \sum_{k=1}^{k_{max}} c_0 p_k v_k \Phi_k dV\right] \cdot \left[\sigma_q c_q c(1-q)dt\right]. \tag{27}$$

Normalized (relative) inversion population of active ion of a saturable absorber $\frac{dq}{dt} = \frac{dN_q}{c_q dV}$ is

$$\frac{dq}{dt} = cc_0\sigma_q(1-q)\sum_{k=1}^{k_{max}} p_k v_k \Phi_k. \tag{28}$$

Introduce now parameter $\beta = cc_0\sigma_q \equiv c\frac{c_0}{c_q}\alpha_q$ and take into account spontaneous decay of excited states with the time constant of τ_q. The final equation is

$$\frac{dq}{dt} = \beta(1-q)\sum_{k=1}^{k_{max}} p_k v_k \Phi_k - \frac{q}{\tau_q}. \tag{29}$$

Intensity of the laser output emission for the k^{th} mode can be estimated as corresponding intracavity photon energy divided by time necessary to let all photons escape through the output coupler:

$$\mathbf{P}_p^{(k)} = \mathbf{N}_p^{(k)} h\nu \frac{1-R_p}{T} \equiv \frac{1-R_p}{T} h\nu c_0 v_k p_k \equiv \frac{1-R_p}{T}\mathbf{Q} v_k p_k, \tag{30}$$

where $\mathbf{Q} = h\nu c_0$.
The set of rate equations for multi-mode laser dynamics with an intracavity sat-

urable element can be presented as follows:

$$\begin{aligned}
&\frac{dn(\vec{r},t)}{dt} = \sigma_D P_D(t)\Phi_D(\vec{r})(1-n(\vec{r},t)) - \chi n(\vec{r},t)\sum_{k=1}^{k_{max}} v_k p_k(t)\Phi_k(\vec{r}) - \frac{n(\vec{r},t)}{\tau_n} \\
&\frac{dp_k}{dt} = \chi p_k \int\limits_V n(\vec{r},t)\Phi_k(\vec{r})dV \\
&- \frac{p_k}{T_p}\left(\rho_p + 2a_q\left[\alpha_q(1-\int\limits_V q(\vec{r},t)\Phi_k(\vec{r})dV) + \gamma_q\int\limits_V q(\vec{r},t)\Phi_k(\vec{r})dV\right]\right) \\
&\frac{dq}{dt} = \beta(1-q)\sum_{k=1}^{k_{max}} p_k v_k \Phi_k - \frac{q}{\tau_q}
\end{aligned} \tag{31}$$

The laser output power (measured in $Watts$) is:

$$\mathbf{P}_p^{(k)} = \frac{1-R_p}{T_p}\mathbf{Q}v_k p_k \tag{32}$$

where

$$\begin{aligned}
\sigma_D = \frac{u}{h\nu c_0}, \qquad \chi = cc_0\sigma_s, \qquad \rho_p = -\mathbf{ln}R_p, \\
\alpha_q = c_q\sigma_q, \qquad \gamma_q = c_q\sigma_\gamma, \qquad \beta = cc_0\sigma_q, \\
\mathbf{Q} = h\nu c_0 \quad [J/m^3], \\
\alpha_q a_q \equiv -\mathbf{ln}T_q, \qquad \gamma_q a_q \equiv -\mathbf{ln}T_\gamma
\end{aligned}$$

We choose now typical material parameters for investigation of laser dynamics: $c_0 = 1.36\cdot 10^{20}cm^{-3}$ ($Nd^{3+}:YAG$, 1% doping), $\sigma_s = 28\cdot 10^{-20}cm^2$ (the Nd emission cross section at 1064 nm), $c_q = 6.44\cdot 10^{17}cm^{-3}$ (the Cr density in $Cr^{4+}:YAG$), $\sigma_q = 5\cdot 10^{-18}cm^2$ (Cr absorption cross section at 1064 nm; from ground state), $\sigma_\gamma = 1.59\cdot 10^{-19}cm^2$ (Cr absorption cross section at 1064 nm; from upper state), the diode pump wavelength $\lambda_D = 808nm$, the laser wavelength $\lambda = 1064nm$, the laser crystal length $a_c = 20mm$, the saturable absorber crystal length $a_q = 5mm$, $\sigma_D = 0.03[cm^3J^{-1}]$, the output coupler reflection $R_p = 0.5$ ($\rho_p = 0.69$), $\chi = 1140ns^{-1}$,$T_q = 0.2$,$T_\gamma = 0.95$, $\alpha_q = 3.22cm^{-1}$, $\gamma_q = 0.1cm^{-1}$, $\beta = 2.04\cdot 10^4 ns^{-1}$, $\mathbf{Q} = 25.4Jcm^{-3}$.
We assume also (for practical purposes) the following: all variables are constant along the cavity axis, the default mode volume is the same for all modes. These assumptions are equivalent to:
$\Phi_k(\vec{r}) = \frac{1}{a_c}\Phi_k(x,y)$ ($k = D, 1\cdots k_{max}$), $v_k = a_c S$, $S = \pi w_0^2/4$, where w_0 is the Gaussian diameter of the TEM_{00} mode of the cavity).

With these assumptions the laser dynamics equations are:

$$\frac{dn(x,y,t)}{dt} = \frac{\sigma_D}{a_c} P_D(t)\Phi_D(x,y)[1-n(x,y,t)] \tag{33}$$
$$- \chi n(x,y,t) S \sum_{k=1}^{k_{max}} p_k(t)\Phi_k(x,y,t) - \frac{n(x,y,t)}{\tau_n}$$

$$\frac{dp_k(t)}{dt} = \chi p_k(t) \int_S n(x,y,t)\Phi_k(x,y)dS \tag{34}$$
$$- \frac{p_k(t)}{T_p}\left(\rho_p + 2a_q\left[\alpha_q(1 - \int_S q(x,y,t)\Phi_k(x,y)dS) + \gamma_q \int_S q(x,y,t)\Phi_k(x,y)dS\right]\right)$$

$$\frac{dq(x,y,t)}{dt} = \beta(1-q(x,y,t))S\sum_{k=1}^{k_{max}} p_k(t)\Phi_k(x,y) - \frac{q(x,y,t)}{\tau_q} \tag{35}$$

$$\mathbf{P}_p^{(k)}(t) = \frac{1-R_p}{T_p}\mathbf{Q}a_c S p_k(t) \tag{36}$$

$$\sigma_D = \frac{u}{h\nu c_0}, \qquad \chi = cc_0\sigma_s, \qquad \rho_p = -\mathbf{ln}R_p, \qquad \alpha_q = c_q\sigma_q,$$
$$\gamma_q = c_q\sigma_\gamma, \qquad \beta = cc_0\sigma_q, \qquad \mathbf{Q} = h\nu c_0, \qquad \alpha_q a_q \equiv -\mathbf{ln}T_q, \qquad \gamma_q a_q \equiv -\mathbf{ln}T_\gamma$$

It is useful also to define the gain coefficient $g(t)$:

$$g(t) = \frac{d}{dt}\mathbf{ln}[p(t)]. \tag{37}$$

If $g(t) = const$ during $t \subseteq [t_1, t_2]$, then $p(t_2) = p(t_1)e^{g(t_2-t_1)}$. Assuming $t_2 - t_1 = T_p/2$ (time of a single path of laser photons through the laser cavity) we can define the gain factor:

$$K_a = \frac{1}{2}gT_p \tag{38}$$

In case of negligible intracavity losses we can estimate the gain coefficient for a k^{th} mode

$$G_k(t) = \frac{1}{2}g_k(t)T_p \equiv \frac{1}{2}\chi T_p \int_V n(\vec{r},t)\Phi_k(\vec{r})dV. \tag{39}$$

In a laser with cylindrical symmetry, the transversal mode pattern is given[4] by combination of a Gaussian beam profile and a Laguerre polynomial. The modes are denoted TEM_{pl} where p and l are integers labeling the radial and angular

[4]See, for example, $http://en.wikipedia.org/wiki/Transverse\_mode$

mode orders, respectively. The intensity at a point $[\vec{r}, \phi]$ (polar coordinates) is given by:

$$I_{pl}(r, \phi) = I_0 \rho^l \left[L_p^l(\rho)\right]^2 \cos^2(l\phi) e^{-\rho}, \tag{40}$$

where $\rho = 2r^2/w^2$, the parameter w is the spot size of the mode corresponding to the Gaussian beam radius, and L_p^l is the associate Laguerre polynomial of order p and index l:

$$L_n^k(x) = (-1)^k \frac{d^k}{dx^k} \left[L_{n+k}(x)\right] = \frac{1}{n!} e^x x^{-k} \frac{d^n}{dx^n}(e^{-x} x^{n+k}). \tag{41}$$

The first few Laguerre polynomials are:

Table 1

p	$L_p^k(x)$
0	1
1	$-x + 1 + k$
2	$\frac{1}{2}\left(x^2 - 2(k+2)x + (k+1)(k+2)\right)$
3	$\frac{1}{3!}\left(-x^3 + 3(k+3)x^2 - 3(k+2)(k+3)x + (k+1)(k+2)(k+3)\right)$
4	$\frac{1}{4!}(-x^4 - 4(k+4)x^3 + 6(k+3)(k+4)x^2 -$ $- 4(k+2)(k+3)(k+4)x + (k+1)(k+2)(k+3)(k+4))$

The absorption parameter α and the initial transmission T_q of the saturable absorber are related as follows

$$e^{-\frac{\alpha}{T}t} = (T_q^2)^{\frac{t}{T}} \rightarrow \alpha = 2 \log \frac{1}{T_q} \tag{42}$$

There is also an absorption parameter γ due to upward transitions from the excited quantum states of the laser crystal. Corresponding absorption coefficient is $\gamma = -2 \log T_\gamma$ where T_γ is the transmission of the bleached crystal. Contrast of the saturable absorber is defined as

$$K = \frac{1 - T_q}{1 - T_\gamma} \tag{43}$$

If initial absorption changes (due to thicker crystal or increased Cr^{4+} ion concentration) then we assume that value of γ changes proportionally to α. If the

number of active centres in a saturable absorber changes (due to change either of their density or just of the size of the crystal), then both parameters (α and γ) must be changed proportionally.
Dynamic transmission of the saturable absorber $T^{(q)}(x,y)$ can be obtained from the expression above by replacing $\alpha \Rightarrow \alpha(1-q)+\gamma q$. We obtain

$$T^{(q)}(\vec{r},t) = e^{-\frac{1}{2}(\alpha(1-q(\vec{r},t))+\gamma q(\vec{r},t))} \equiv T_q^{1-q(\vec{r},t)} T_\gamma^{q(\vec{r},t)} \tag{44}$$

This formula can be used to calculate transversal transmision of the saturable absorber as a function of time. The following parameters are used in the above equations: the one round-trip loss for a k-mode: $\rho_k = -\log R_k \equiv -\log[(1 - q_p^{(k)})R_p$, decay constants τ_n (for spontaneous inverse population emission) and τ_q (for saturable absorber inverse population lifetime); the gain parameter χ of the fundamental frequency in the activated laser crystal, excitation rate factor $\sigma(t)$ for active laser ions caused by the diode pump, the parameter α of the fundamental frequency absorption in a saturable absorber, and the parameter β of the saturable absorber transition rate caused by photon absorption. The fundamental frequency seeding emission $\epsilon_p(t)$ has its origin in quantum fluctuations and is considered spatially uniform. Initial conditions for the set of equations are:

$$n(\vec{r},0) = p(\vec{r},0) = q(\vec{r},0) = 0 \tag{45}$$

3 Determining laser cavity modes

The set of optical modes to be used in the numerical model is defined by the Gaussian diameter w of the fundamental mode TEM_{00} and by the list of higher order modes with indexes $[pl]$. Parameter w is calculated on the basis of special algorithm where beam path inside the cavity is modelled by using the **ABCD** matrix method[5]. A Gaussian beam at any point is defined by the complex parameter q :

$$\frac{1}{q} = \frac{1}{R} - \frac{i}{\pi w^2} \tag{46}$$

where R is the beam wave front curvature radius. If q is defined, then

$$w = \frac{1}{\sqrt{-\pi \Im(\frac{1}{q})}} \qquad R = \frac{1}{\Re(\frac{1}{q})} \tag{47}$$

[5]See, for example, *http : //en.wikipedia.org/wiki/Ray_transfer_matrix*

The propagation of the laser beam through intracavity components (left mirror, laser crystal, Q-switch crystal, right mirror) is calculated on the basis of the following formula:

$$q_B = \Phi(q_A, \mathbf{M}^{(\rightarrow)}) \equiv \frac{q_A M_{11}^{(\rightarrow)} + M_{12}^{(\rightarrow)}}{q_A M_{21}^{(\rightarrow)} + M_{22}^{(\rightarrow)}} \tag{48}$$

where q_A is the beam parameter at the left mirror

$$\frac{1}{q_A} = \frac{1}{R_1} - \frac{i}{\pi w_0^2}, \tag{49}$$

R_1 is the radius of curvature of the 1^{st} mirror, and w_0 is a zero iteration beam diameter. The matrices are as follows. Transfer matrix from mirror 1 to mirror 2):

$$\mathbf{M}^{(\rightarrow)} = \begin{bmatrix} M_{11}^{(\rightarrow)} & M_{12}^{(\rightarrow)} \\ M_{21}^{(\rightarrow)} & M_{22}^{(\rightarrow)} \end{bmatrix} = M^{(R_1)} \times M^{(a)} \times M^{(R_2)} \tag{50}$$

Matrix for the spherical mirror:

$$\mathbf{M}^{(R)} = \begin{bmatrix} 1 & 0 \\ -\frac{2}{R} & 1 \end{bmatrix} \tag{51}$$

Matrix for intracavity crystals:

$$\mathbf{M}^{(a)} = \begin{bmatrix} 1 & a \cdot n_{YAG} \\ 0 & 1 \end{bmatrix} \tag{52}$$

The beam travel in opposite direction is given by

$$\mathbf{M}^{(\leftarrow)} = \begin{bmatrix} M_{11}^{(\leftarrow)} & M_{12}^{(\leftarrow)} \\ M_{21}^{(\leftarrow)} & M_{22}^{(\leftarrow)} \end{bmatrix} = M^{(R_2)} \times M^{(a)} \times M^{(R_1)} \tag{53}$$

Finally, one round trip is defined by the matrix

$$\mathring{\mathbf{M}} = \mathbf{M}^{(\rightarrow)} \times \mathbf{M}^{(\leftarrow)} \tag{54}$$

Algorithm:

1. Set

$$q^{(0)} = \frac{1}{\frac{1}{R_1} - \frac{i}{\pi w_0^2}} \tag{55}$$

w_0 is an arbitrary zero iteration beam diameter

2. Repeat $q^{(j)} = \Phi(q^{(j-1)}, \mathring{\mathbf{M}}), \qquad j = 1, 2, \cdots$
   until $|w^{(j)} - w^{(j-1)}| < \eta, \quad$ where η is the required accuracy.

Using the Gaussian beam waist diameter w we can define all high-order transversal modes $I_{pl}(r, \phi)$ for a given laser cavity. Each optical mode may have aperture losses due to laser crystal limited diameter. The relative loss for one path through the cavity for a k^{th} mode can be calculated as follows

$$\zeta_k = \int\limits_{\vec{r} \notin S} \Phi^{(k)}(\vec{r}) d^2\vec{r}. \tag{56}$$

At a given energy, the modes of higher order have lower peak intensities and higher losses due to increasing of mode spatial spread as indexes $[p, l]$ increase. The commonly used parameter for a multi mode beam quality can be defined as

$$\mathbf{M}^2 = \left(\frac{d^*}{w}\right)^2, \tag{57}$$

where d^* is the width of the transversal distribution (at the level of e^{-1}) of the beam intensity which is given by

$$\sum_{k=1}^{n} p_k \Phi^{(k)}(\vec{r}). \tag{58}$$

4 Examples of laser simulation

We chose typical material parameters:

Table 2

Initial Q-switch absorption	$\alpha = 4.41$
Residual Q-switch absorption	$\gamma = 0.04$
Laser crystal gain parameter	$\chi = 20$
Q-switch excitation parameter	$\beta = 80$
Diode pump power parameter	$\sigma = 0.36$
Energy scaling factor	$Q = 0.15$
Output coupler reflection	$R_p = 0.5$
Intracavity losses[6]	$q_p = 0.005$
Cavity round trip time	$T = 0.473$
Diode maximal current	$I_D^{max} = 125A$
Diode threshold current	$I_D^{th} = 25A$
Active laser crystal ion lifetime	$\tau_n = 230\mu s$
Q-switch crystal ion lifetime	$\tau_q = 8.5\mu s$
Laser rod diameter	$a = 3mm$

Simulation examples will be presented for two case studies:

Table 3

	LaserA	**LaserB**
Fundamental laser mode waist	$w = 0.39 \ \ mm$	$w = 0.57mm$

4.1 Results of the simulation (laser A: free-running regime)

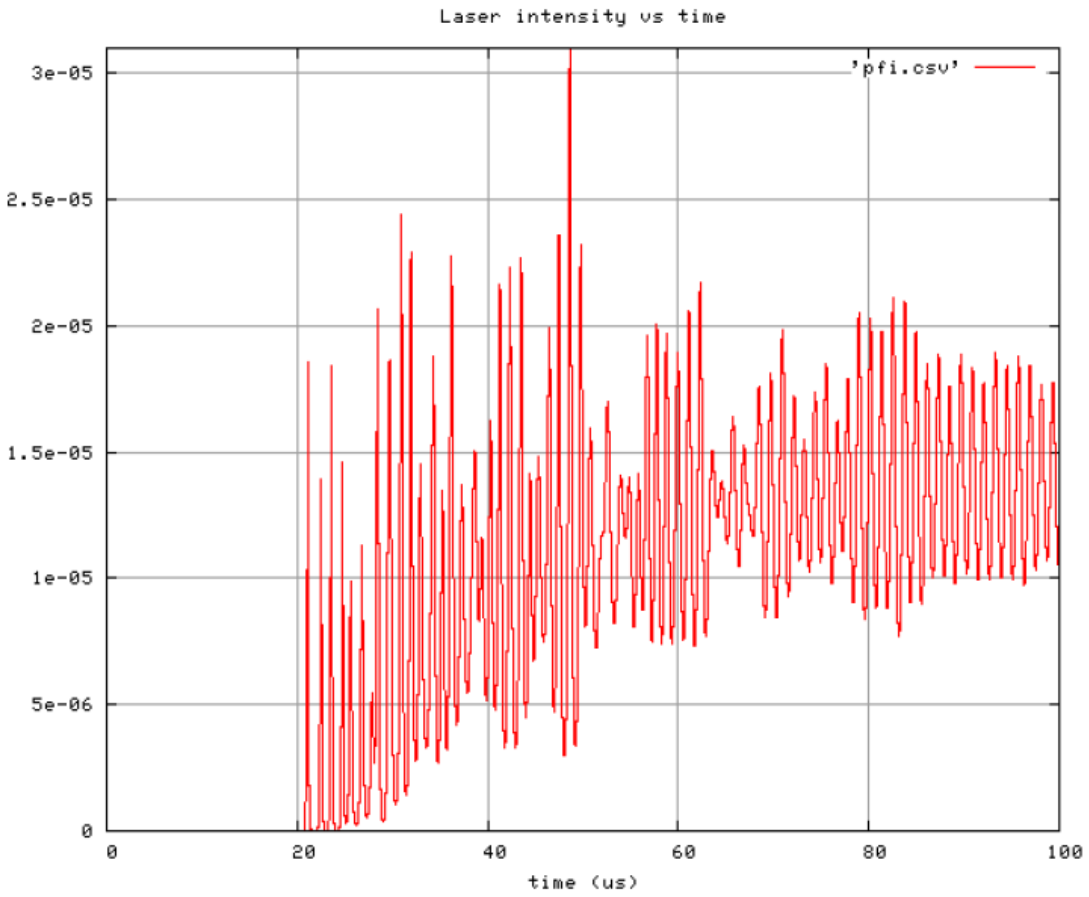

Figure 2: A typical random-pulsed lasing

Lasing in Figure 2 is presented at the beginning. Intensity "fluctuations" are caused both by basic laser dynamics and multimode competition processes.

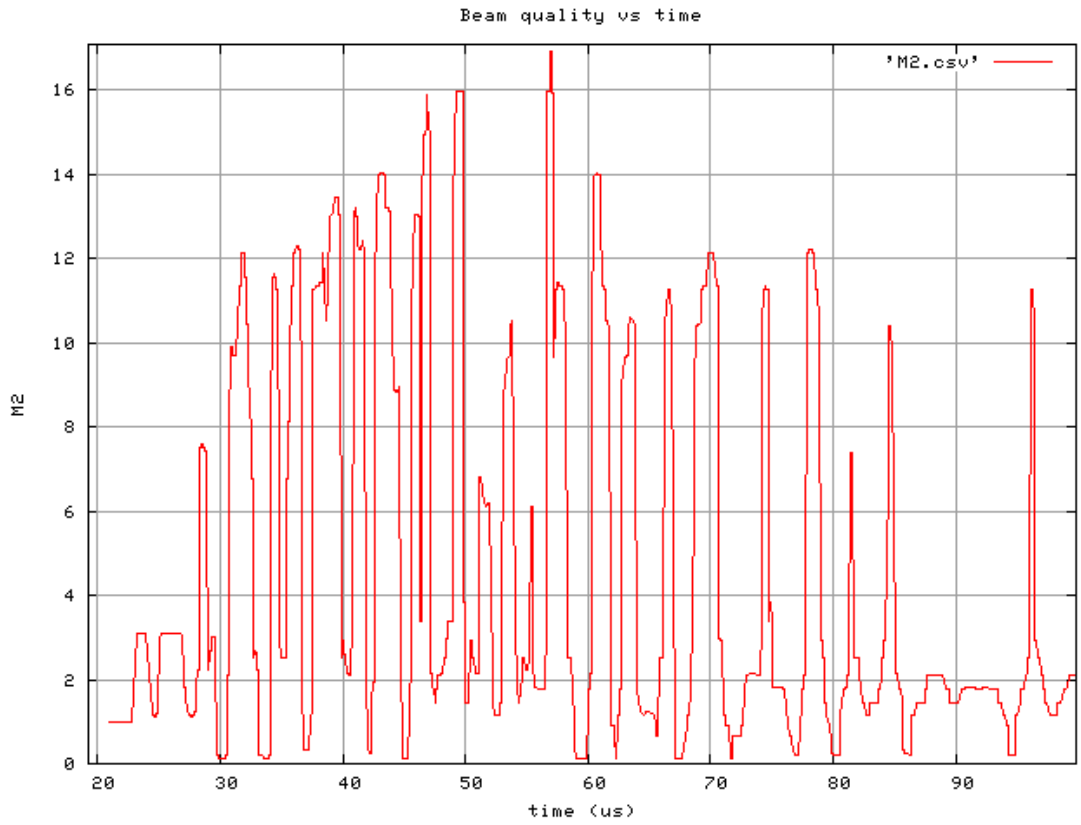

Figure 3: The beam quality parameter

The beam quality parameter M^2 illustrates in Figure 3 the multimode lasing which starts from the TEM_{00} mode ($M^2 = 1$) followed by generation of higher order modes.

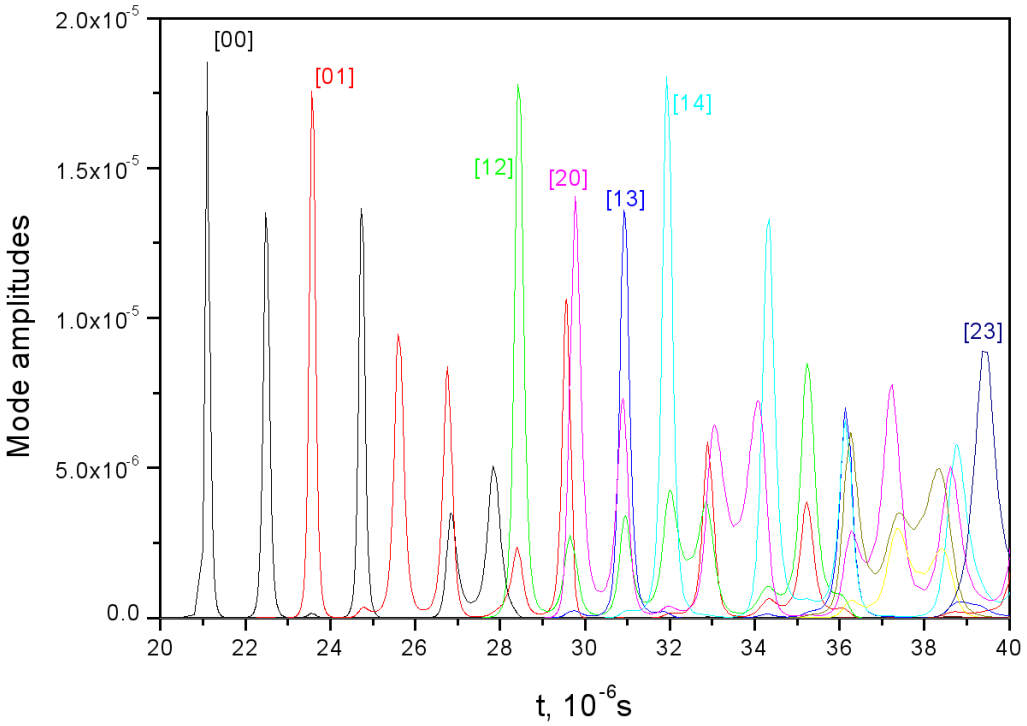

Figure 4: "Competition" of cavity modes during first $20\mu s$ after reaching laser threshold

Note in Figure 4 that lasing starts from a [00] mode and later several modes are being generated simultaneously.

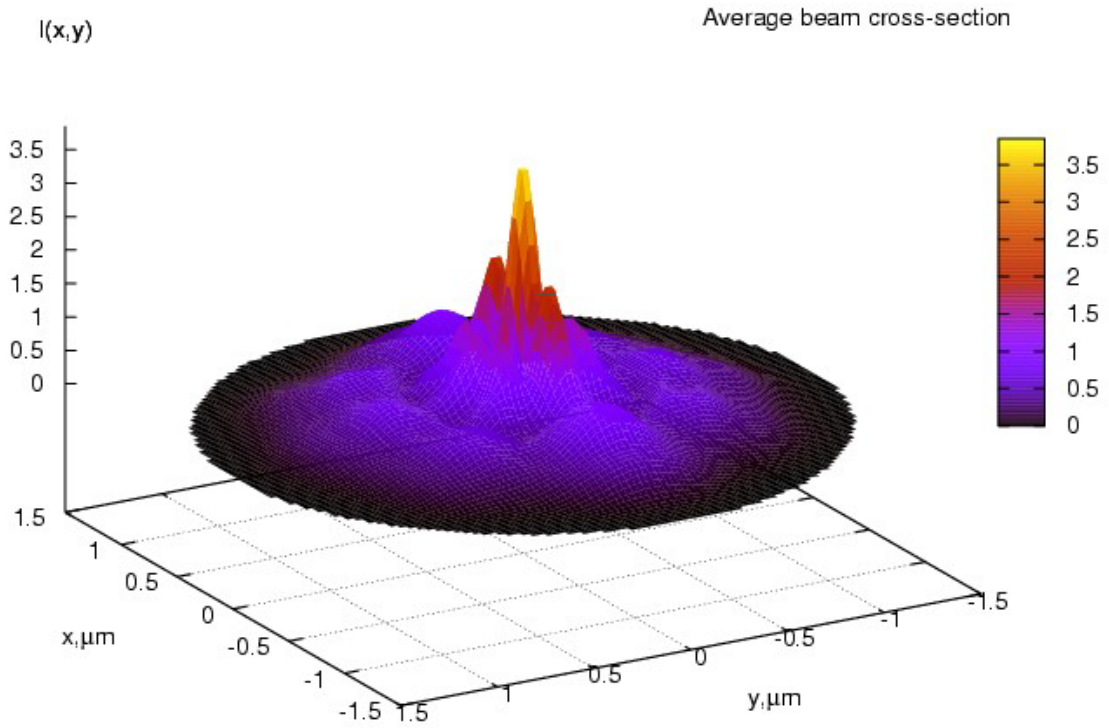

Figure 5: Laser beam transversal distribution (averaged over the whole lasing time period).

Note in Figure 5 that transversal expansion to higher-order modes is limited by the laser rod diameter.

4.2 Results of the simulation (laser A: Q-switched regime)

Results of the simulation of the laser **A** in its actual configuration (with the saturable absorber) are presented in Figures 6, 7, 8, 9 . The only one pulse is produced.

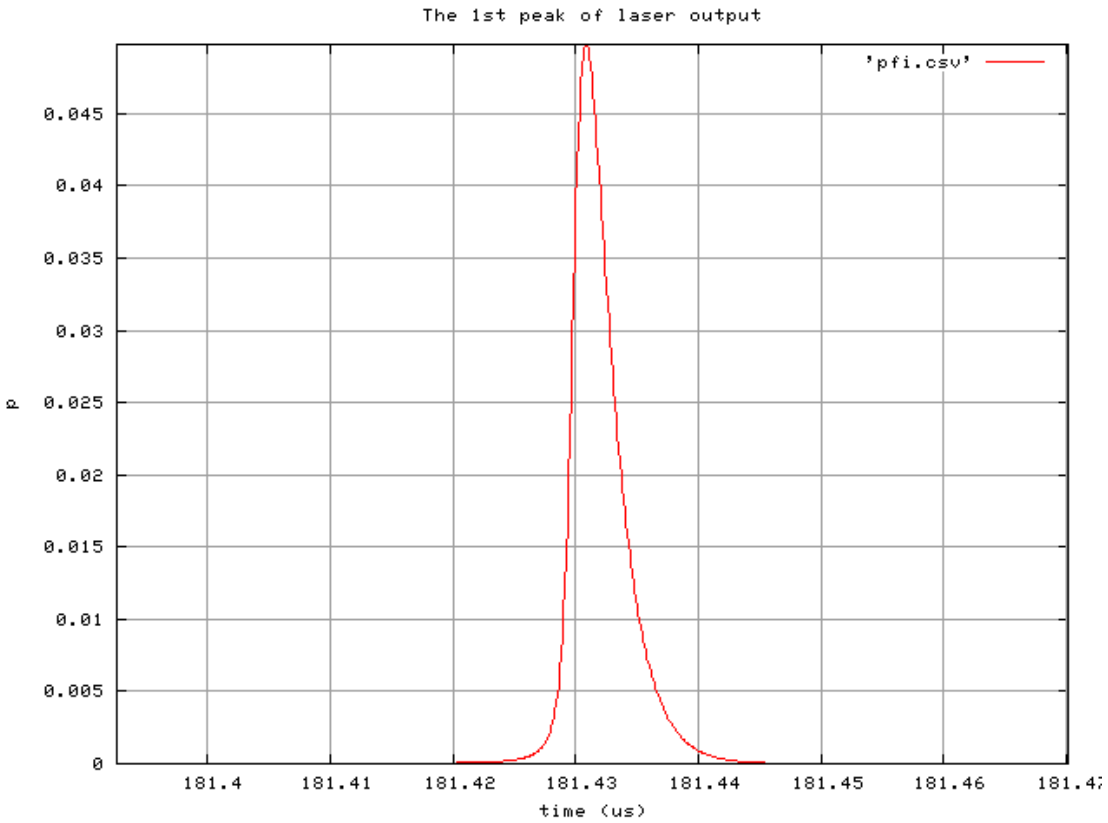

Figure 6: A single laser 3-ns pulse is generated in the Q-switched regime.

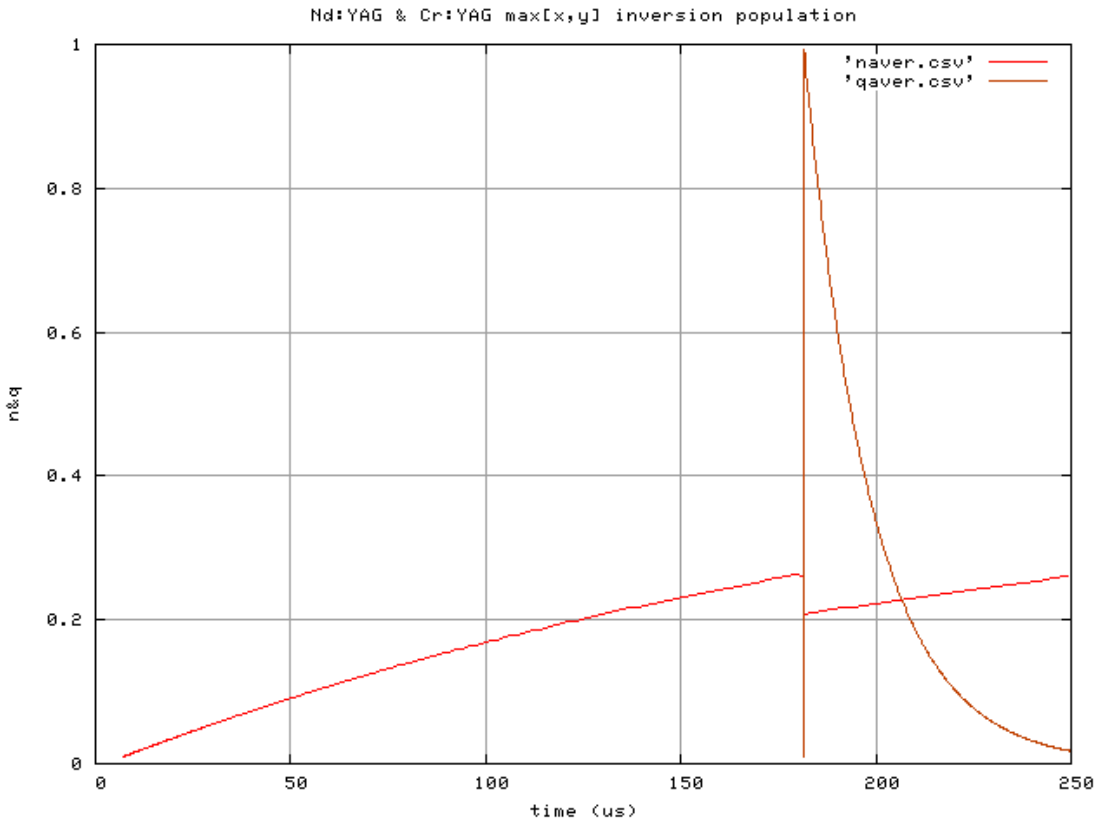

Figure 7: $Nd:YAG$ (red curve) and $Cr:YAG$ (brown curve) max$[x,y]$ inversion population

Inverse population of the laser crystal and the $Cr:YAG$ crystal versus time demonstrate slow increase of the gain until the lasing threshold, and rapid "switch" during laser pulse generation (Figure 7).

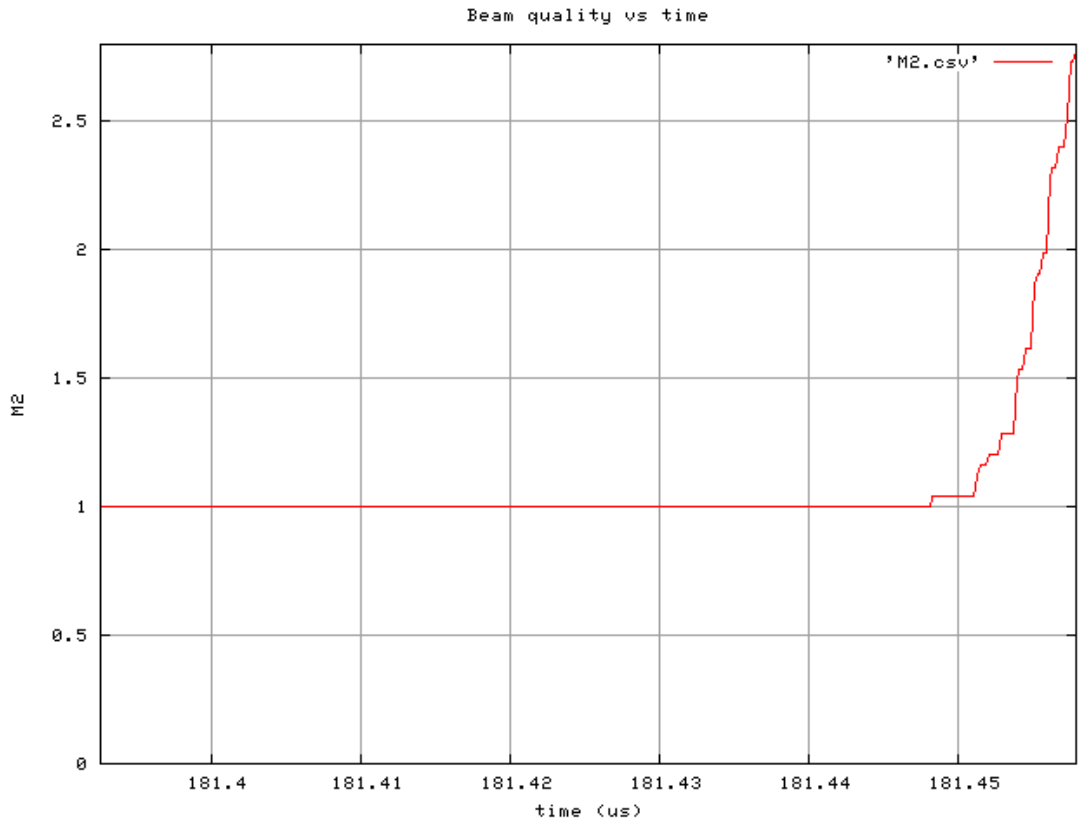

Figure 8: Laser beam quality in the Q-switched regime

Laser beam quality in the Q-switched regime (Figure 8) is $M^2 = 1$ (TEM_{00} mode) during main laser output (181.42 – 181.45μs) . Deterioration of the output beam quality is insignificant (it takes place when output intensity is less then 1% of its maximum).

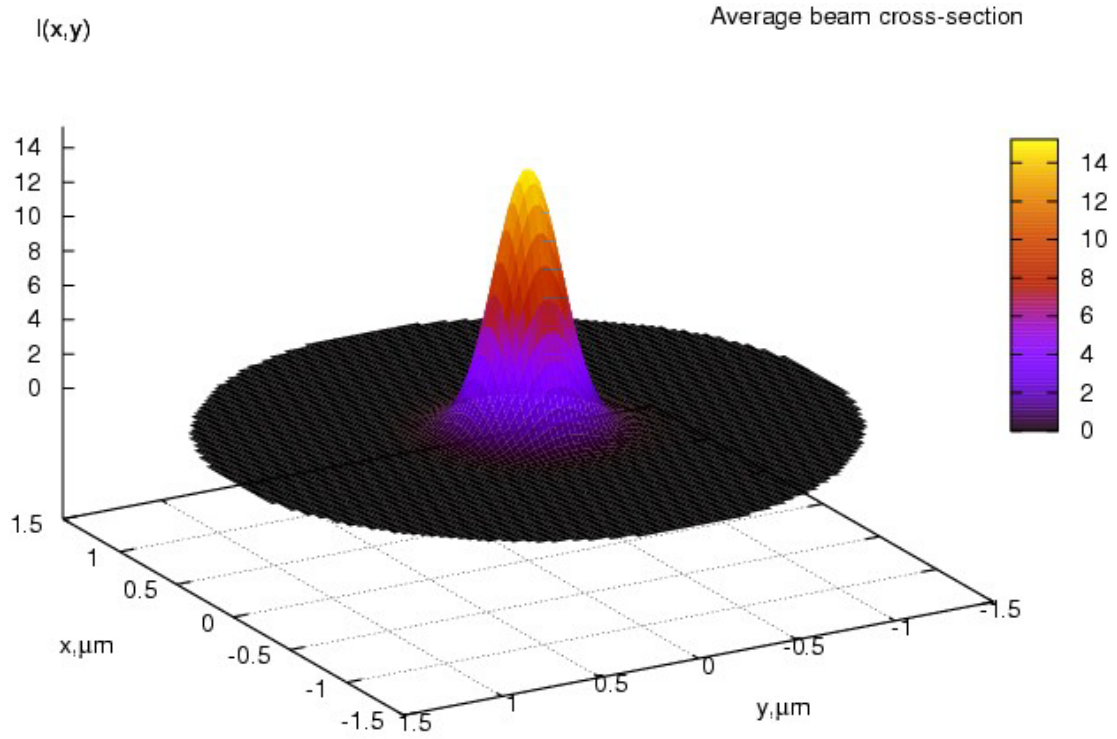

Figure 9: Laser pulse spatial cross section

Laser pulse generated has purely Gaussian shape (Figure 9). As expected, in the Q-switched regime the only mode generated is the TEM_{00} mode. All modes of higher order either do not reach the threshold or are unable to bleach the saturating absorber.

4.3 Results of the simulation (laser B: free-running regime)

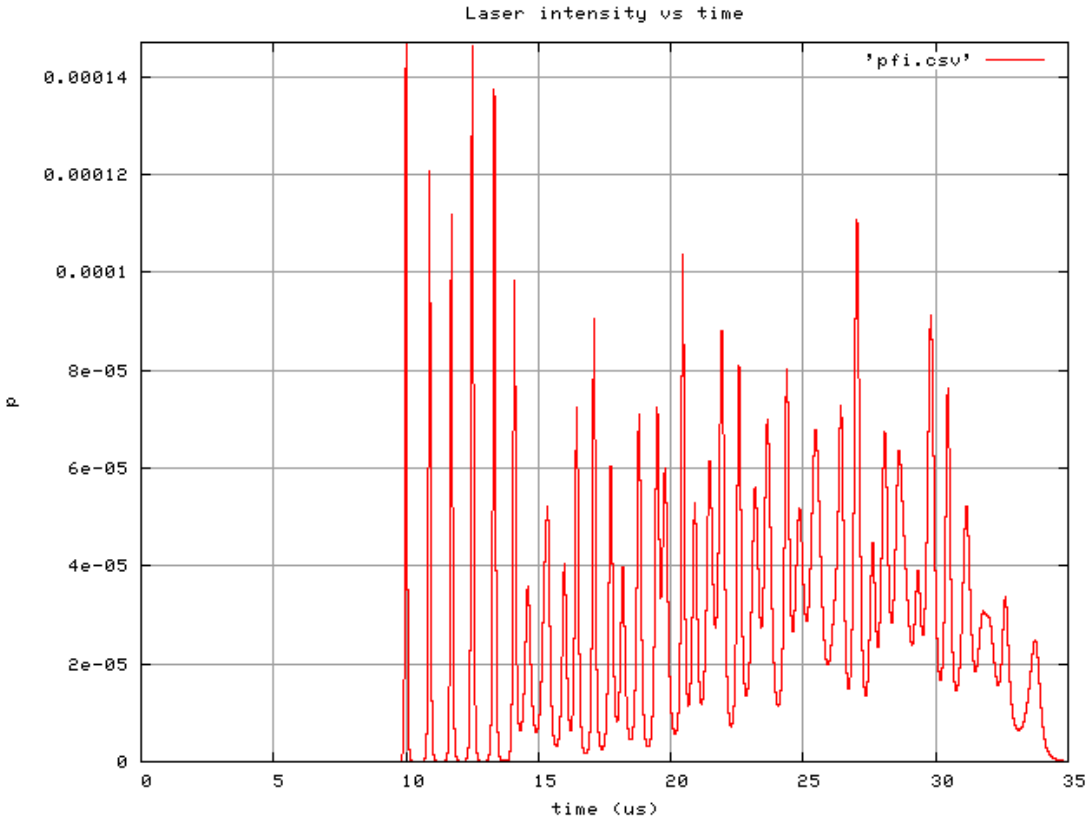

Figure 10: Typical random-pulsed lasing

A typical random-pulsed lasing (presented in Figure 10 for the 1^{st} $35\mu s$. Intensity "fluctuations" are caused both by basic laser dynamics and multimode competition processes.

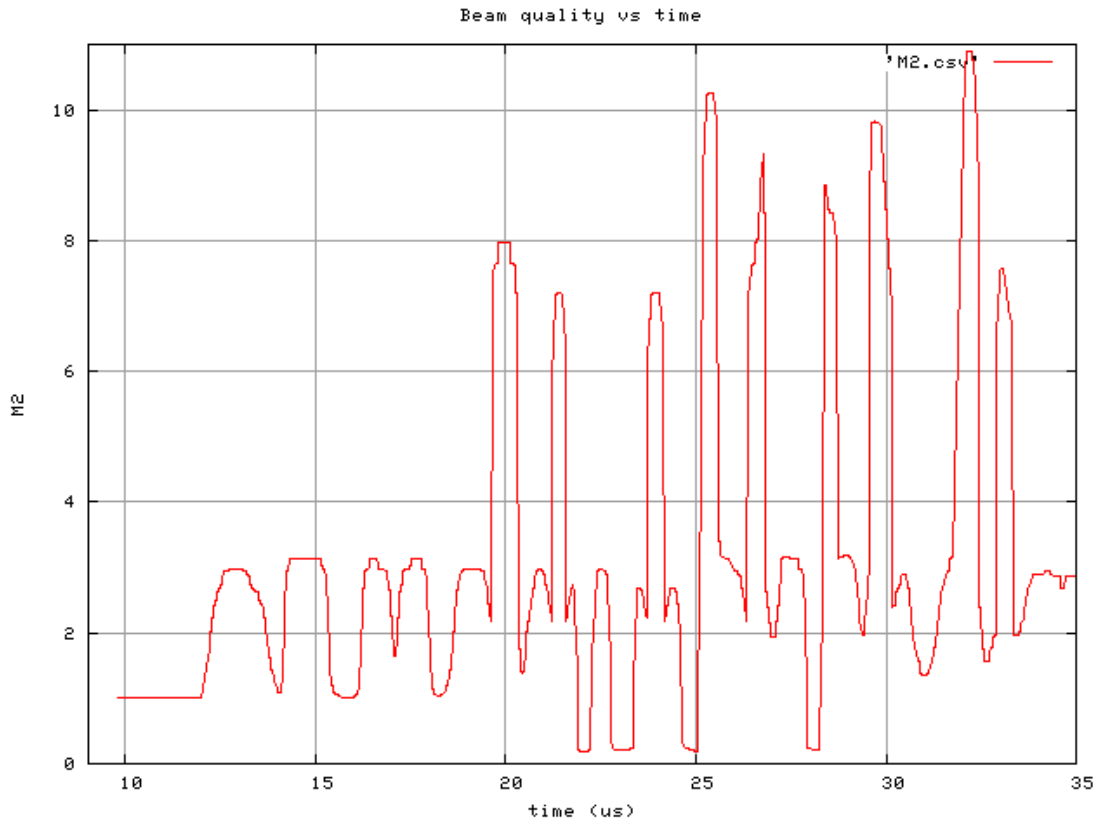

Figure 11: The beam quality parameter M^2 (laser B)

The beam quality parameter M^2 illustrates multimode lasing which starts from the TEM_{00} mode ($M^2 = 1$) followed by generation of higher order modes (Figure 11).

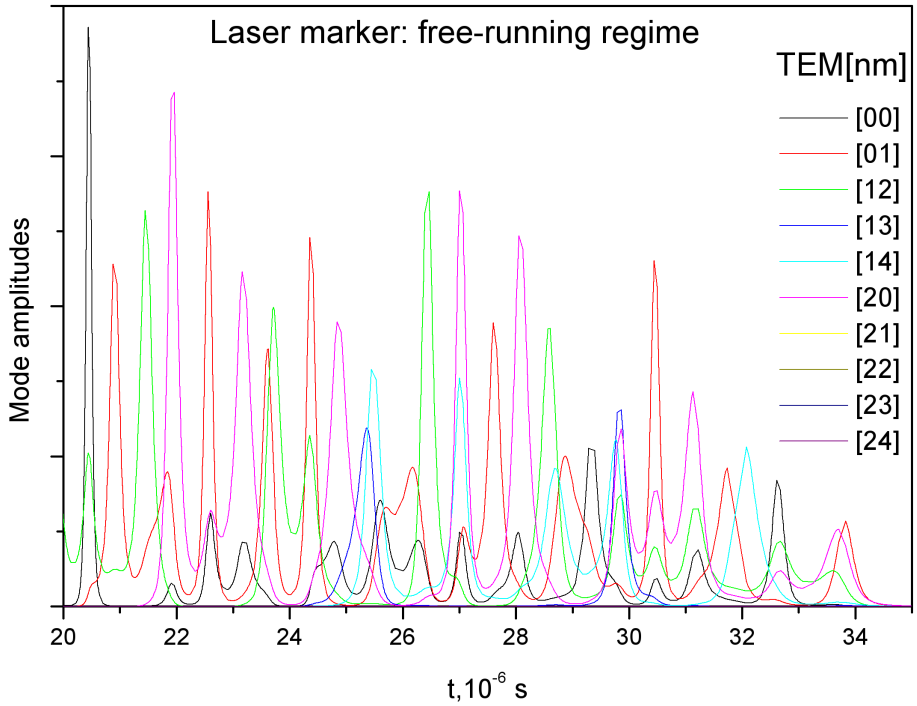

Figure 12: "Competition" of cavity modes (laser B)

"Competition" of cavity modes during first $20\mu s$ after reaching laser threshold (Figure 12).

Figure 13: Laser beam transversal distribution (laser B)

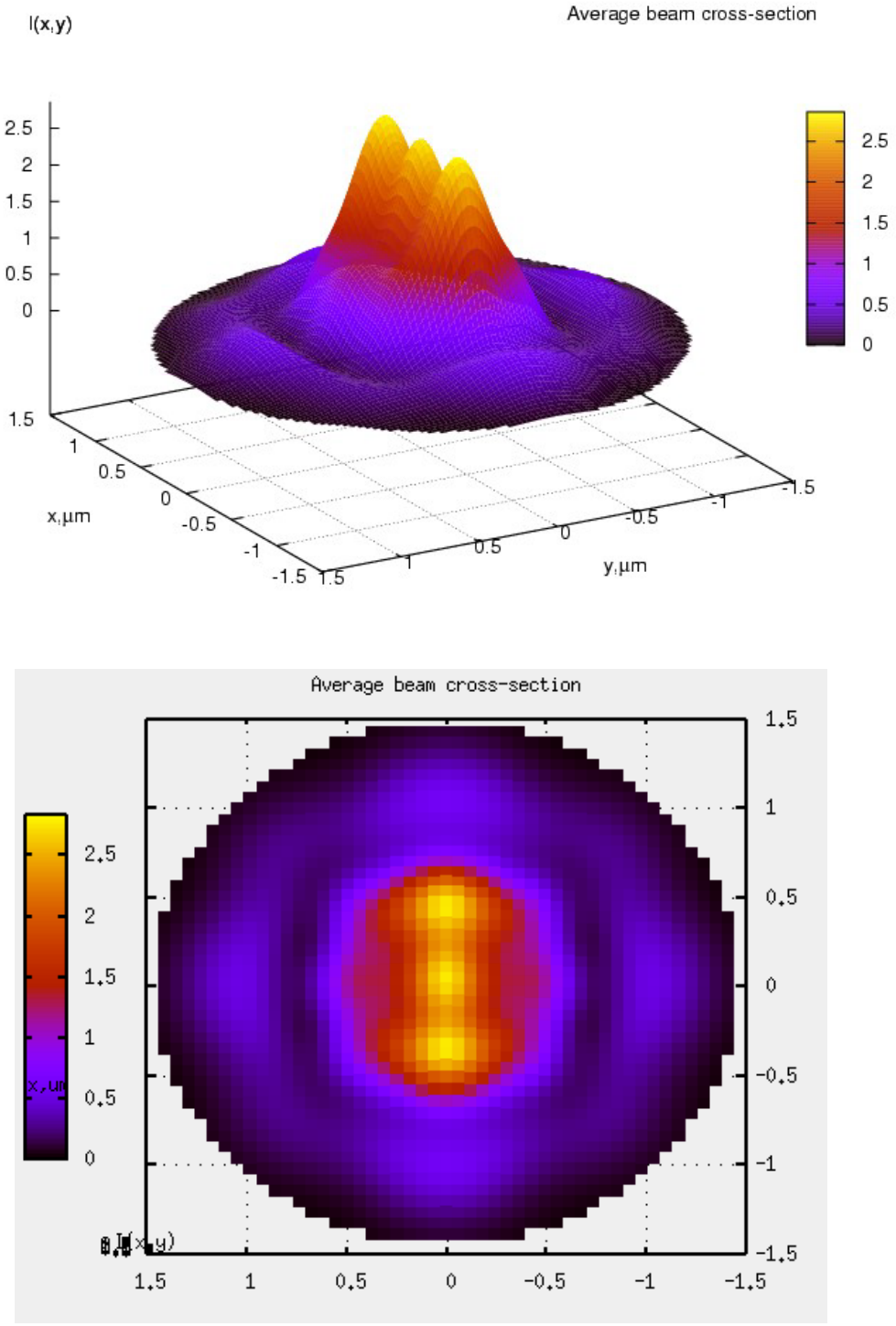

Laser beam transversal distribution (averaged over the whole lasing time period). Note that transversal expansion to higher-order modes is limited by the laser rod diameter (Figure 13).

4.4 Results of the simulation (laser B: Q-switched regime)

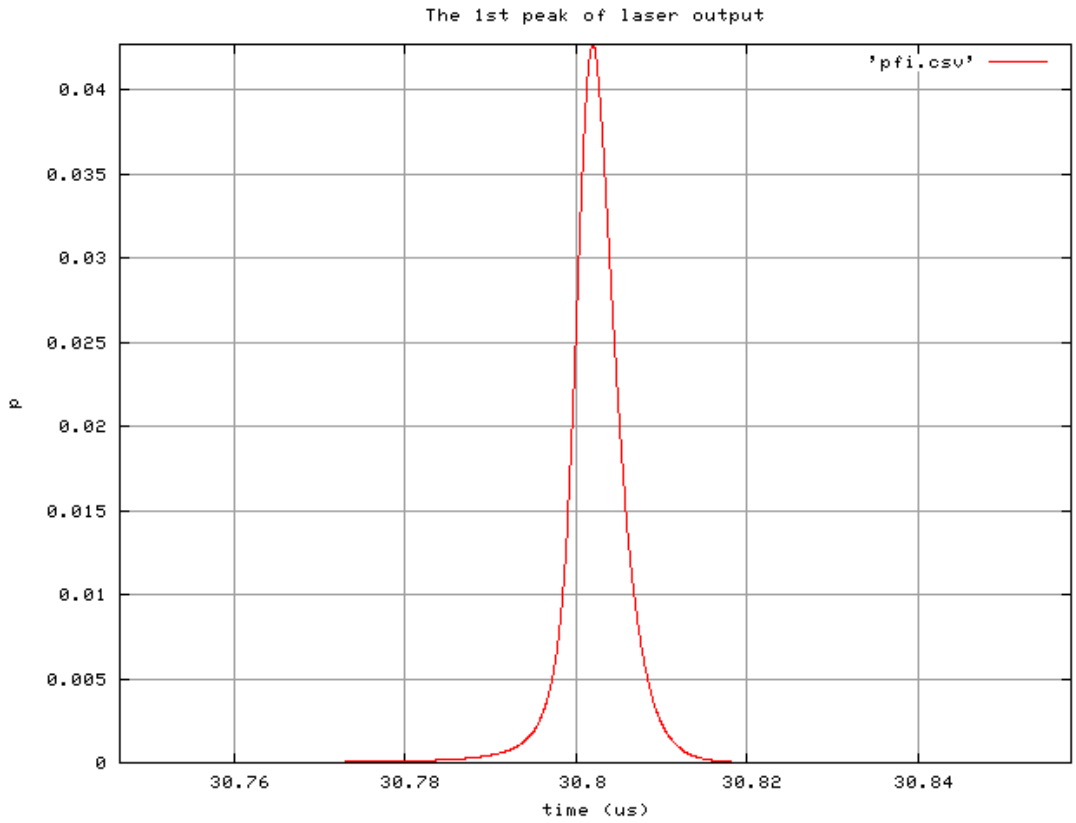

Figure 14: Laser pulse in the Q-switched regime (laser B)

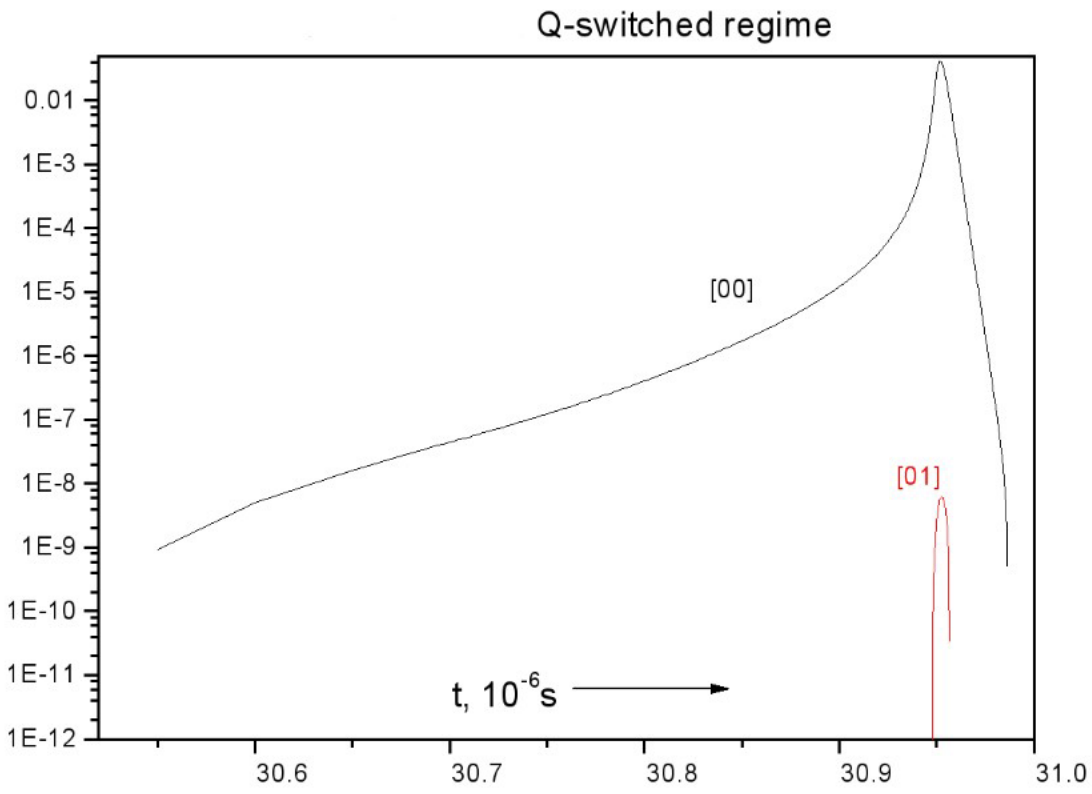

Figure 15: Laser pulse amplification from the quantum noise level (laser B)

Note in the Figure 15 the failed attempt of the [01] mode to enter the game.

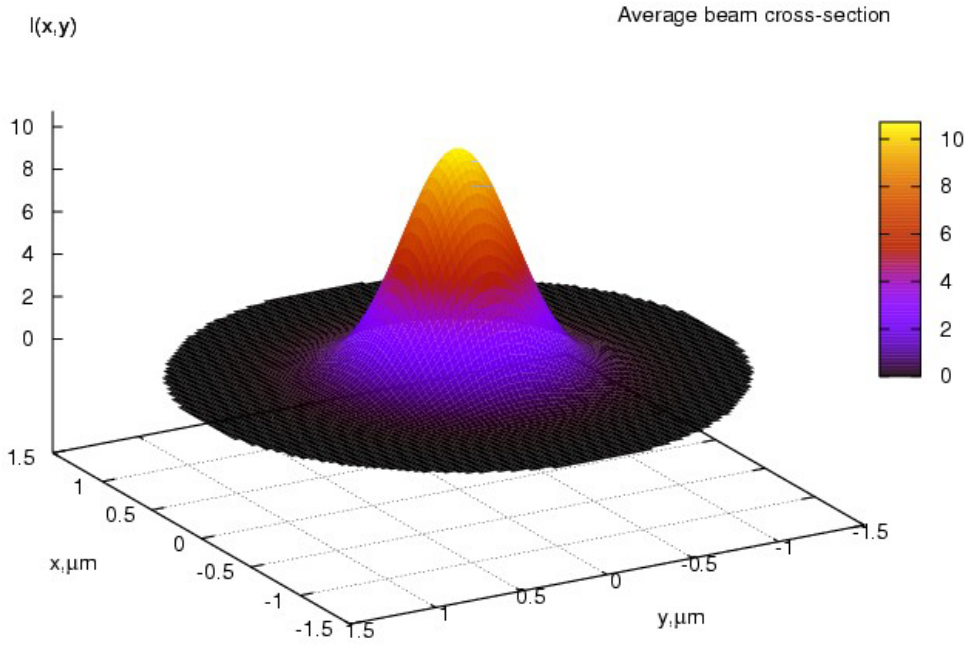

Figure 16: Laser output beam transversal distrtibution (laser B)

The laser B (Q-switched) pulse is purely Gaussian (Figure 16).

4.5 Results of the simulation (laser B: Q-switch, continuous pumping)

The next numerical experiment is to illustrate how mode dynamics of a laser can change in case of a very long pump pulse. In this case a train of Q-switched pulses will be produced. Pulses will be separated by time periods sufficient to pump up the laser crystal to reach the lasing threshold. The train of laser pulses in a Q-switched laser with a long pumping pulse is presented in Figure 17. Simulation results demonstrate that it is the case: pulses are produced with approximately $20\mu s$ periods. It is important to note that intensities of pulses fluctuate (in the range of 1 to 10). Explanation of this behavior can be derived from the next graph.

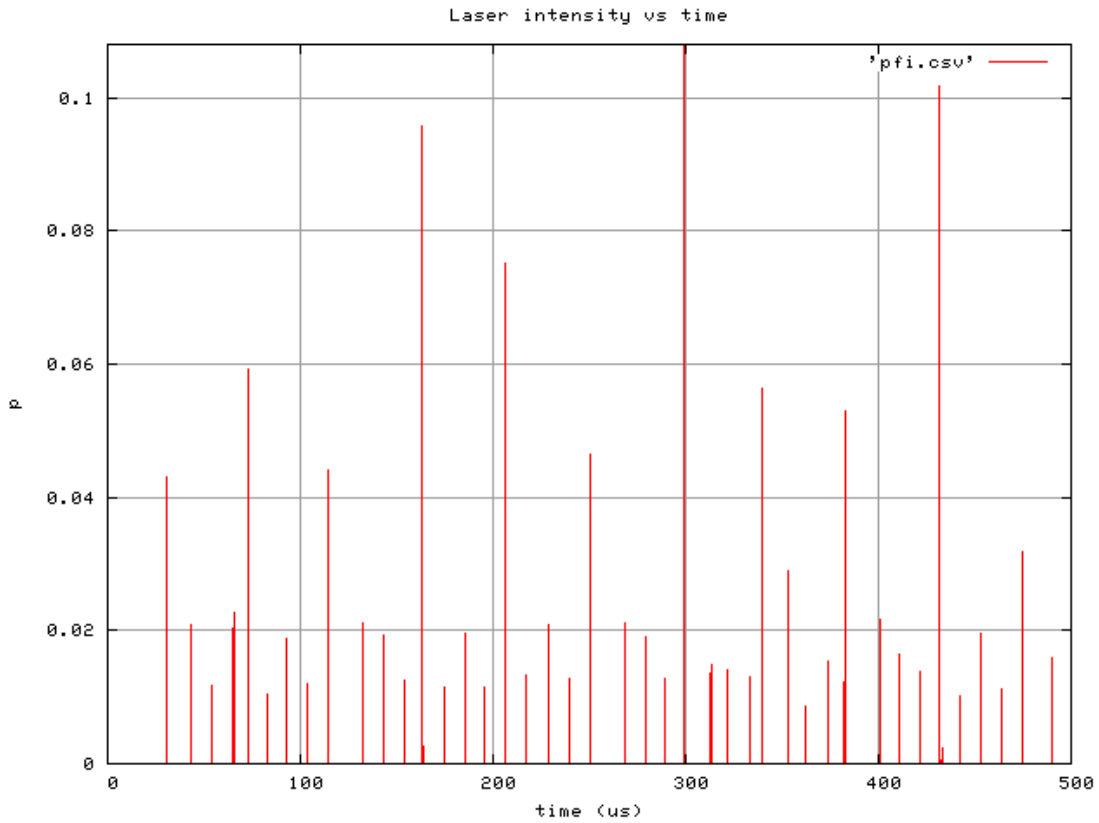

Figure 17: Train of laser pulses in a Q-switched laser with a long pumping pulse (laser B)

Simulation results demonstrate that it is the case: pulses are produced with approximately $20\mu s$ periods. It is important to note that intensities of pulses fluctuate (in the range of 1 to 10). Explanation of this behavior can be derived from the next graph (Figure 18).

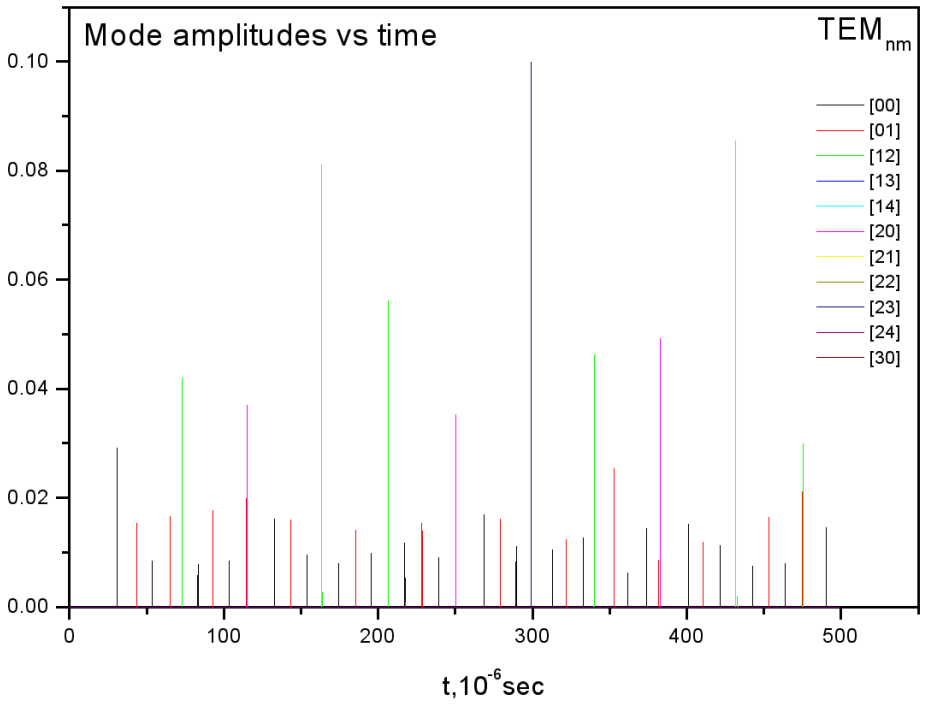

Figure 18: Mode amplitudes versus time in case of a long pumping pulse (laser B)

In case of a long pumping pulse every next laser Q-switched pulse belongs to a different cavity mode. Every next pulse uses different cavity mode because the spatial distribution of the gain in the laser crystal changes with every next pulse. As a result, the average beam quality deteriorates (in this example $M^2 = 2.46$ for pump pulse duration of $150\mu s$).
The beam average transversal distribution is similar to the case of non-Q-switched laser regime, but peak intensities are obviously much higher (Figure 19).

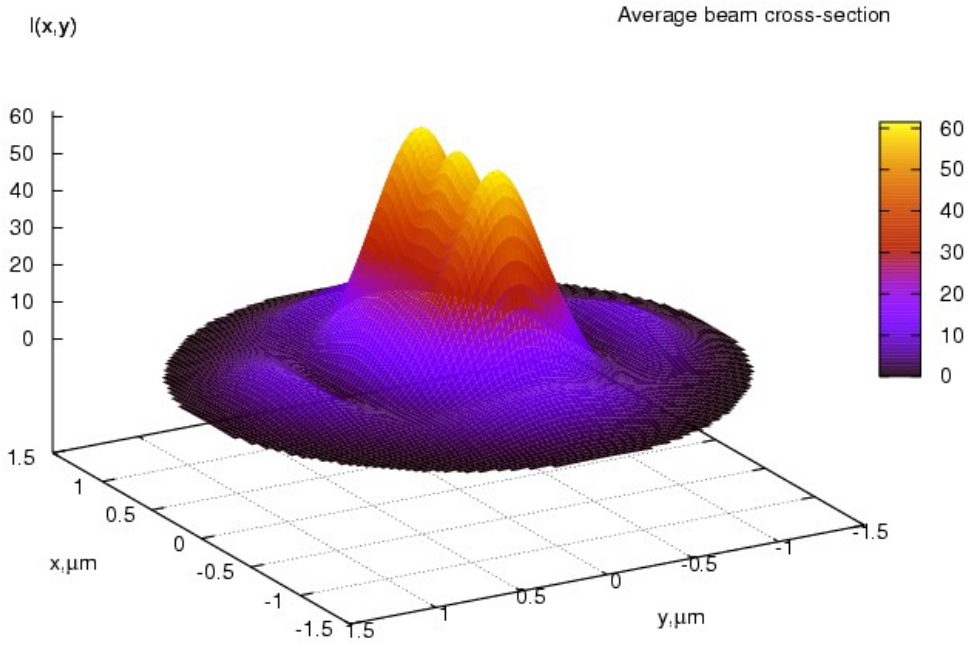

Figure 19: Average beam cross-section in case of Q-switched laser with a $150\mu s$ pump pulse length (laser B)

If losses of all modes except TEM_{00} are made high artificially, then the only mode remaining will be TEM_{00} with the regular period of $14\mu s$.

5 Laser modes and thermal lens effect

Pumping of the laser crystal creates thermal lens which modifies the cavity optical modes. We assume that a lens with optical strength f^{-1} is located between the laser crystal and the passive Q-switch crystal. The **ABCD** matrices must be changed as follows

$$\mathbf{M}^{(\rightarrow)} = M^{(R_1)} \times M^{(a)} \times M^{(th)} \times M^{(R_2)} \tag{59}$$

$$\mathbf{M}^{(\leftarrow)} = M^{(R_2)} \times M^{(th)} \times M^{(a)} \times M^{(R_1)} \tag{60}$$

$$\tag{61}$$

where the matrix associated with the thermal "lens" is:

$$\begin{bmatrix} 1 & 0 \\ -f^{-1} & 1 \end{bmatrix} \tag{62}$$

The optical strength of the thermal lens is roughly proportional to the average absorbed pump power. Illustration of the thermal lens effect in case of initial non-stable optical cavities is presented in Figure 20.

Laser A The flat/concave $1800mm$ cavity ($R_1 = \infty, R_2 = -1.8m$) is non-stable. Thermal lens effect provides stabilization of the cavity mode when pump absorption is high enough to cause focusing with $f < 1.81m$. The change of thermal lens focus from $1.75m$ to $1.80m$ increases mode diameter from $0.8mm$ to $1.6mm$ and mode losses - from 0.07% to 2.6% per round trip.

Laser B The convex/concave cavity ($R_1 = 1m$, $R_2 = -0.7m$) is not stable. In this case thermal lens must be such that $f < 2.63m$. The change of thermal lens focus from 2.50 m to 2.61 m causes mode diameter increase from 0.75 mm to 1.1 mm, and mode losses grow from 0.04% to 2.5% per round trip.

Figure 20: Dependence of the laser mode waist size and mode losses versus thermal lens focus

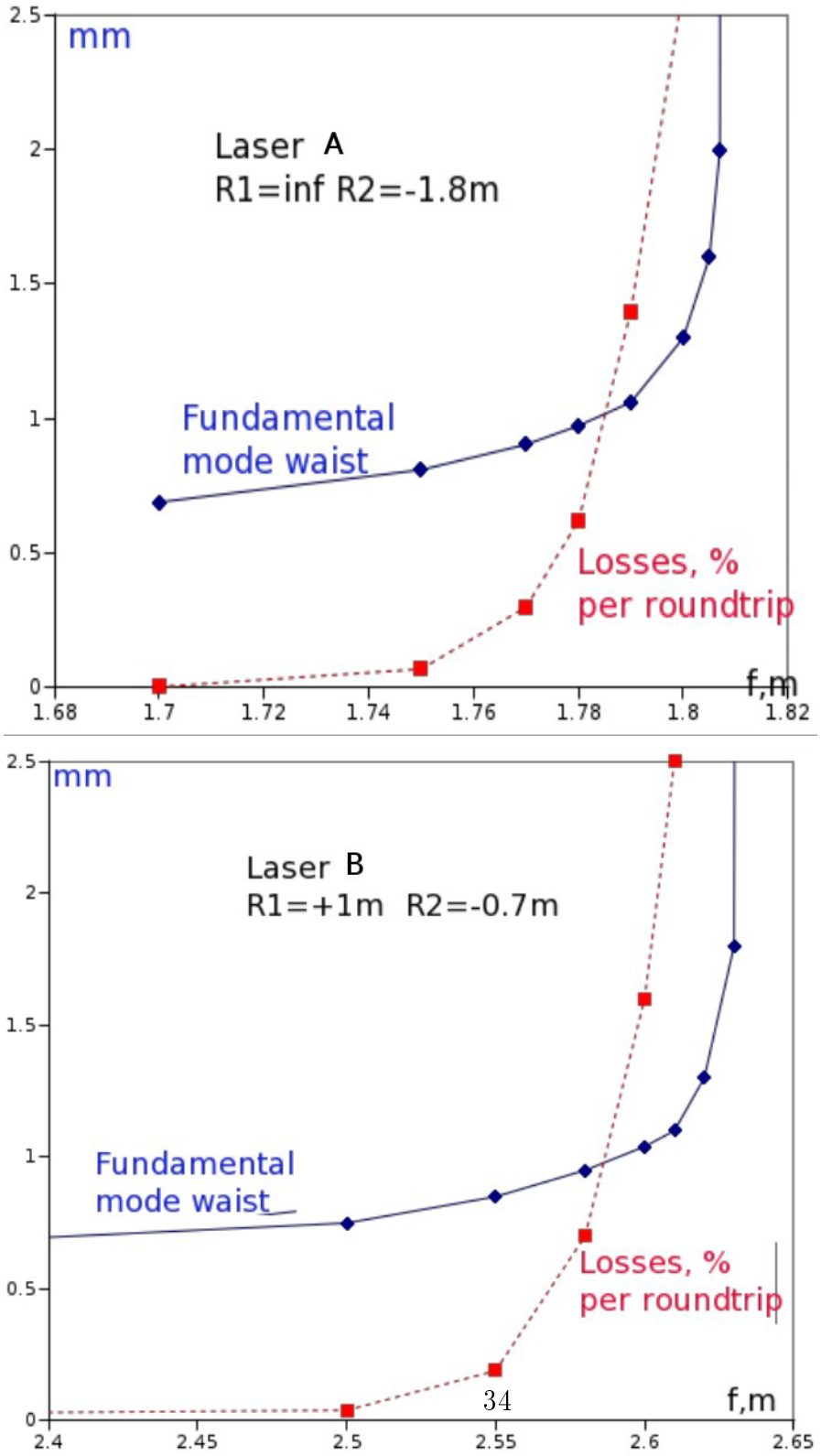

It is important to keep pump power stable because power drift of just 2% can increase mode losses dramatically and even shift to the range of optical mode instability.

6 Summary

- Stimulated emission in the $Nd:YAG$ laser with a saturable absorber $Cr:YAG$ is modelled as a superposition of interacting optical modes which are stable in a given optical cavity
- The interaction of the active laser crystal and a passive Q-switch with diode pump and optical cavity modes is modelled with account of transversal two-dimentional variation of the pump field and of all participating optical modes
- Each elementary volume of an active laser crystal and the Q-switching crystal interacts with all modes (therefore modes are non-linearly linked to each other), and every optical mode interacts with the whole laser crystal. This interaction is given by rate equations. Total number in this set of equations is given by the following formula

  $$N_e = 2k_{max}j^2_{max}$$

  where k_{max} is number of cavity modes and j^2_{max} is the total number of elementary volumes representing intracavity crystals. Most of simulation experiments presented in this paper were done with $N_e = 2 \cdot 10^5$ ($k_{max} = 20$, $j^2_{max} = 100 \times 100$).
- Special numerical tools were used to accelerate calculations without loss of precision.
- Simulation experiments for two laser devices provide quantitative validation of some experimentally observed effects (domination of the fundamental mode in a Q-swithed regime, multimode operation without Q switch) and predict performance of a laser with long pump pulses (trains of laser Q-switched pulses with pule-to-pulse mode switching).

7 References

Yuri Yashkir. Laser micromachining with passively q-switched intra cavity harmonic generator. *SPIE*, TD01:462–466, 2002.

Yuri Yashkir. Pulse shape control in a dual cavity laser: numerical modeling. *Solid State Lasers and Amplifiers II, Proc. of SPIE*, 6190(619018), 2006a. Edited by Alphan Sennaroglu.

Yuri Yashkir. Numerical modeling of the phase-conjugate laser with an intra-cavity stimulated brillouin scattering mirror: Q-switching mode. *Solid State Lasers and Amplifiers II, Proc. of SPIE*, 6190(6190A), 2006b. Edited by Alphan Sennaroglu.

Yuri Yashkir and Qiang Liu. Experimental and theoretical study of the laser micro-machining of glass using high- repetition-rate ultrafast laser. *Solid State Lasers and Amplifiers II, Proc. of SPIE*, 6190(6190V), 2006. Edited by Alphan Sennaroglu.

Yuri Yashkir and Henry van Driel. Passively q-switched 1.57-μm intra cavity optical parametric oscillator. *Applied Optics*, 38:2554–2559, 1999.

Yuri Yashkir and Yuriy Yashkir. Numerical modeling of the intra cavity stimulated raman scattering as a source of sub nanosecond optical pulses. *Proceedings of SPIE - 5460, Solid State Lasers and Amplifiers*, pages 220–227, 9 2004. Alphan Sennaroglu, James G. Fujimoto, Clifford R. Pollock, Editors.

Yuri Yashkir, Marc Nantel, and Bernard Hockley. Numerical simulation of the laser dynamics and laser/matter interactions, and its applications for laser micro-machining. *International Journal of Applied Electromagnetics and Mechanics*, 19:373–377, 2004.